

The Confinement and Breakout of Protostellar Winds: Time-Dependent Solution

Francis P. Wilkin, *IPAC MS 100-22, California Institute of Technology, Pasadena, CA 91125*

Steven W. Stahler, *Astronomy Dept., University of California, Berkeley, CA 94720*

Jets from embedded young stars may be collimated by the anisotropic infall of their cloud envelopes. To model this effect, we have followed numerically the motion of the shocked shell created by the impact of a spherical wind and a rotating, collapsing cloud¹. Quasi-static solutions are found to be dynamically unstable². The present, fully time-dependent calculations include cases both where the wind is driven back by infall to the stellar surface, and where it erupts as a true outflow. For the latter, the time of breakout can be surprisingly late, of order 10^5 yr, at least for wind speeds of 200 km s^{-1} or less. The reason is that the shocked material must be able to climb out of the star's gravitational potential well, carrying with it the dense, swept-up infall. We explore the critical wind speed necessary for breakout as a function of the mass transport rates in the wind and infall, as well as the cloud rotation rate Ω_0 and time since the start of infall. For realistic parameter choices, we do find that breakout can occur. However, these erupting shells do not exhibit the collimation of observed jets, but continue to expand laterally. To halt this expansion, the pressure in the envelope must fall off less steeply than in our model.

References

¹Cassen, P. & Moosman, A. 1981 *Icarus*, 48, 353

²Wilkin, F.P. & Stahler, S.W. 1998 *ApJ*, 502, 661

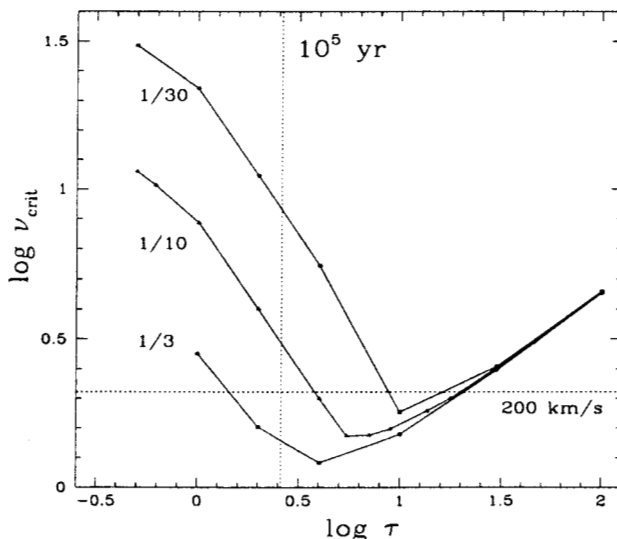


Figure 1: Minimum breakout wind speed versus evolutionary time. The three loci correspond to three ratios of the wind mass loss to infall accretion rate $\alpha = \dot{M}_{wind}/\dot{M}_{infall}$. For a given α , the region above the curve corresponds to breakout, while that below the curve corresponds to recollapse. Fiducials have been indicated for our standard choice of dimensional units, although these nondimensional results may be scaled depending upon cloud rotation rate $\Omega_0 = 10^{-14} \text{ s}^{-1}$, isothermal sound speed $a_0 = 0.2 \text{ km s}^{-1}$, and protostellar (launch) radius $3R_{sun}$.

1. Introduction

We are interested in the influence of the environment on protostellar winds. Can protostellar jets be collimated purely by hydrodynamic effects associated with the anisotropy of matter near the protostar? We investigate this question by assuming no initial collimation of the wind. This is a further development of previous modeling (Wilkin & Stahler 1998, ApJ 502, 661), where self-consistent, quasi-steady, normal force balance solutions for interaction were obtained that grew on an evolutionary, rather than dynamical, timescale. The current work eliminates the assumption of quasi-steady flow and of normal force balance. We consider the initial value problem of a wind launched from the protostellar surface that sweeps up infall and either escapes or is driven back by the combined effects of infall ram pressure and gravity due to the protostar.

2. Formulation

The supersonic collision of the wind and infall lead to the formation of two shocks, an infall and a wind shock. The modest speeds involved ($< 300 \text{ km/s}$ typically) imply efficient post-shock cooling leading to a thin shocked shell, which is described by its radius $R(\theta)$ with surface density $\sigma(\theta)$ and speed $\mathbf{V}(\theta)$, including rotation.

We follow the evolution of this shell including the fluxes of mass and momentum onto it from both sides, as well as gravity due to the star, which is important.

The wind is isotropic, with mass loss rate \dot{M}_{wind} and constant speed V_w .

The infall is that of the inner limit of the inside-out collapse of a singular, isothermal, uniformly rotating sphere of angular speed Ω , according to Cassen & Moosman, with accretion rate $\dot{M}_i = m_0 a_0^3/G$.

The centrifugal radius associated with the infall is $R_{cen} = m_0^3 a_0 \Omega^2 t^3/16$. The infall becomes progressively more spherical at radii larger than R_{cen} .

3. Method of Solution

We solve simultaneous equations for mass conservation and the force law in axisymmetry. The equations in Lagrangian form are

$$\begin{aligned}\frac{D(\ln(\mathcal{A}\sigma))}{Dt} &= [\rho_w w'_n - \rho_i u'_n]/\sigma - \frac{\partial}{\partial \theta} \left(\frac{V_\theta}{R} \right) \\ \frac{D\mathbf{V}_p}{Dt} &= [\rho_w w'_n \mathbf{w}'_p - \rho_i u'_n \mathbf{u}'_p]/\sigma - \frac{GM_*}{R^2} \hat{r} + \frac{V_\theta^2}{R} \hat{\omega} \\ \frac{Dl_s}{Dt} &= -\rho_i u'_n l'_i/\sigma \quad \frac{DR}{Dt} = V_r\end{aligned}$$

where the substantial derivative is

$$\frac{D}{Dt} = \frac{\partial}{\partial t} + \frac{V_\theta}{R} \frac{\partial}{\partial \theta}$$

In these equations, subscript 'p' indicates poloidal part of vector velocity, l indicates specific angular momentum about the axis ($R \sin \theta V_\phi$), and a prime indicates the difference between a given velocity component of the wind or infall and that of the moving shell e.g. $u'_n = u_n - V_n$. Infall velocities are denoted by u , wind velocities by w , and shell velocities by V . The area element per unit polar angle is \mathcal{A} .

The equations are integrated as if they were ordinary differential equations with a Runge-Kutta scheme, and neighboring solutions are differenced to obtain the needed cross-stream derivatives. The shell has 50 angle points that are regridded when necessary due to the drift of points in polar angle towards the midplane.

4. Initial Conditions

We specify the form, as a function of polar angle θ , of the shell radius, mass per unit area, and the three components of velocity within the shell.

The shell is initially spherical and massless, with radius equal to that of the protostar. As the shell evolves it receives mass from both the wind and infall, so an instant after the start of the calculation the shell has a well-defined, finite values for all the physical quantities of interest. The initial velocity of the shell satisfies the force law, which implies normal force balance in the frame of the shell. The initial velocity components of the shell are given by the ratio of the rates at which mass and momentum reach the shell, which for the θ and ϕ components of velocity yields the velocity components of the infall, but diluted by the admixture of mass from the wind.

5. Nondimensional Ratios and Scalings

By nondimensionalizing the equations we are able to efficiently explore parameter space, because the solutions may be scaled in three dimensions. There are three nondimensional ratios that characterize the problem. These are the ratio of wind mass loss rate to infall rate $\alpha = \dot{M}_{wind}/\dot{M}_i$, and a non-dimensional wind speed ν and a nondimensional time τ . All other dimensional variables may be adjusted by scaling the solution - in particular, the protostellar radius does not introduce a new parameter, it is chosen as our length unit L for the nondimensional equations.

The unit of velocity is derived from the free-fall speed at the protostellar surface at a characteristic time. This characteristic time is that when the centrifugal radius equals the protostellar radius. The resulting nondimensional ratios are as follows:

$$\tau = \left(\frac{t}{3.85 \times 10^4 \text{ yr}} \right) \left(\frac{L}{3 R_{sun}} \right)^{-1/3} \left(\frac{a_o}{0.2 \text{ km/s}} \right)^{1/3} \left(\frac{\Omega_o}{10^{-14} \text{ s}^{-1}} \right)^{2/3}$$

$$\nu = 2.10 \left(\frac{V_w}{200 \text{ km/s}} \right) \left(\frac{L}{3 R_{sun}} \right)^{1/3} \left(\frac{a_o}{0.2 \text{ km/s}} \right)^{-4/3} \left(\frac{\Omega_o}{10^{-14} \text{ s}^{-1}} \right)^{1/3}$$

6. Results

We have thoroughly explored the relevant parameter space of solutions and determined the minimum wind speed necessary for breakout (Figure 1). Imagine we have a wind of fixed properties corresponding to a given α and ν . Drawing a horizontal line corresponding to this ν in the figure, this wind can first launch an outflow that will break out at the evolutionary time when the plotted curve for this value of α first intersects the line. The second intersection is not physically relevant, since the wind would already have broken out and cannot be reconfined at a later time.

Sample evolutionary sequences are shown for a case of breakout (Figures 2-4 at bottom) and recollapse (Figures 5 and 6 at right). The only difference between these models is the initial wind speed. Shells that break out are typically quite smooth and regular, but the collapsing shells are highly unstable to rippling. We are not concerned with the detailed properties of such recollapsing shells, because realistically they will not remain intact, but will constantly be interacting with fragments of other shells, if we assume that when the shell impacts the protostar another shell begins to rise at that location.

7. Conclusions

We have determined the parameter range necessary for breakout of an initially spherically-symmetric wind from rotating infall. From this it is possible to determine the evolutionary time at which breakout may first occur for given system parameters of wind and infall.

The breakout time is surprisingly late, due to the gravitational force exerted on the shocked material. The shell must not only have greater ram pressure support from the wind than confinement from infall, but must be able to climb out of the gravitational potential well.

The breakout time would presumably be significantly reduced if: 1) the wind were more collimated; 2) the wind were launched from a disk at larger radius than that of the protostar; 3) the shell fragments, allowing some wind to escape but some shocked material to fall back in; 4) the shocked wind and infall do not mix, but a shearing layer is present. In this way it would be possible for shocked wind to break out yet shocked infall would not be carried outward.

Although the shells become extended along the rotational axis, they do not achieve a jet-like geometry. The thin shell analysis of this work is unable, however, to show crossing shock-like behavior, if it occurs. At late times, the shell becomes progressively more spherical due to the spherical distribution of matter far beyond the centrifugal radius.

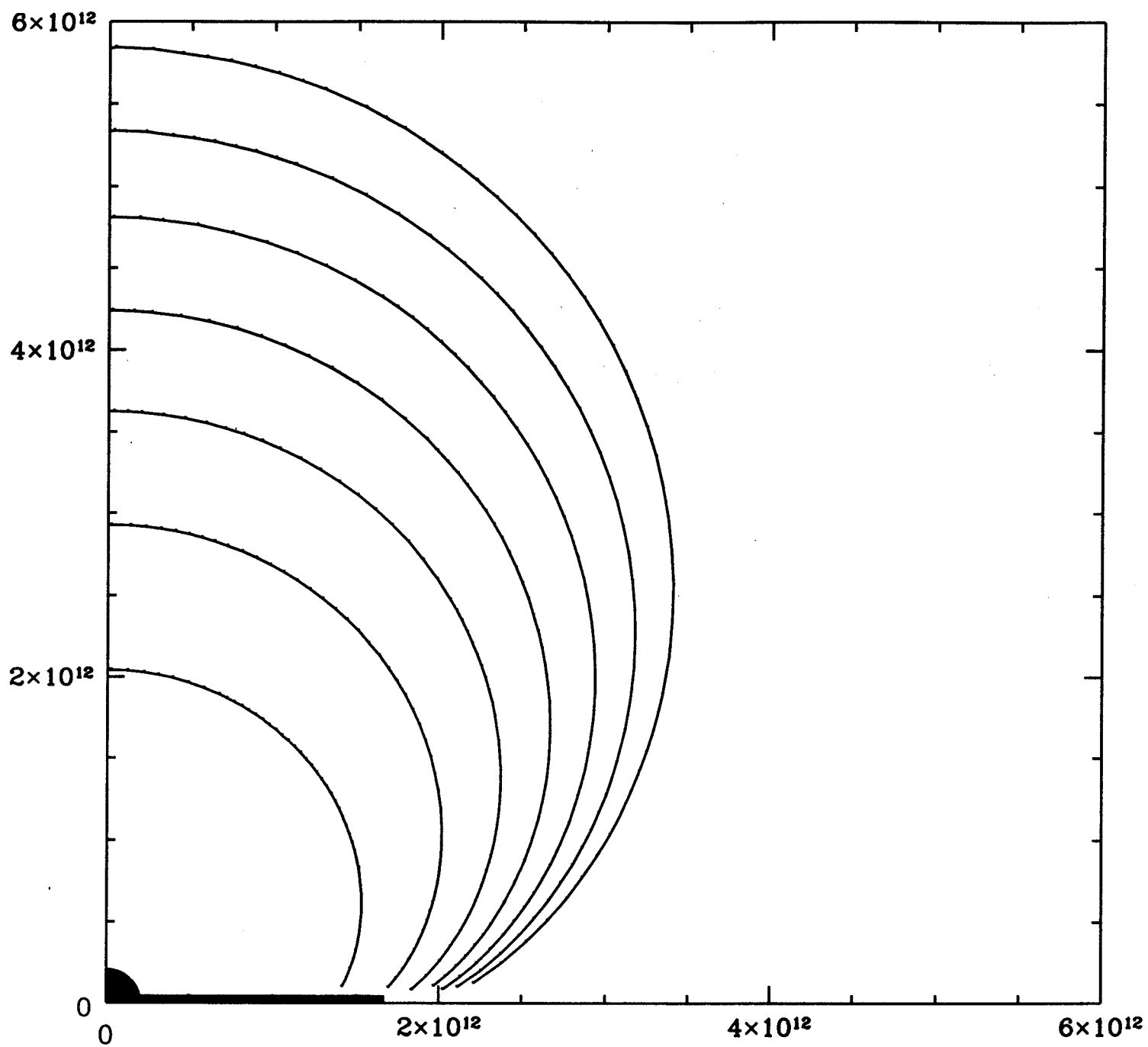


Fig 2

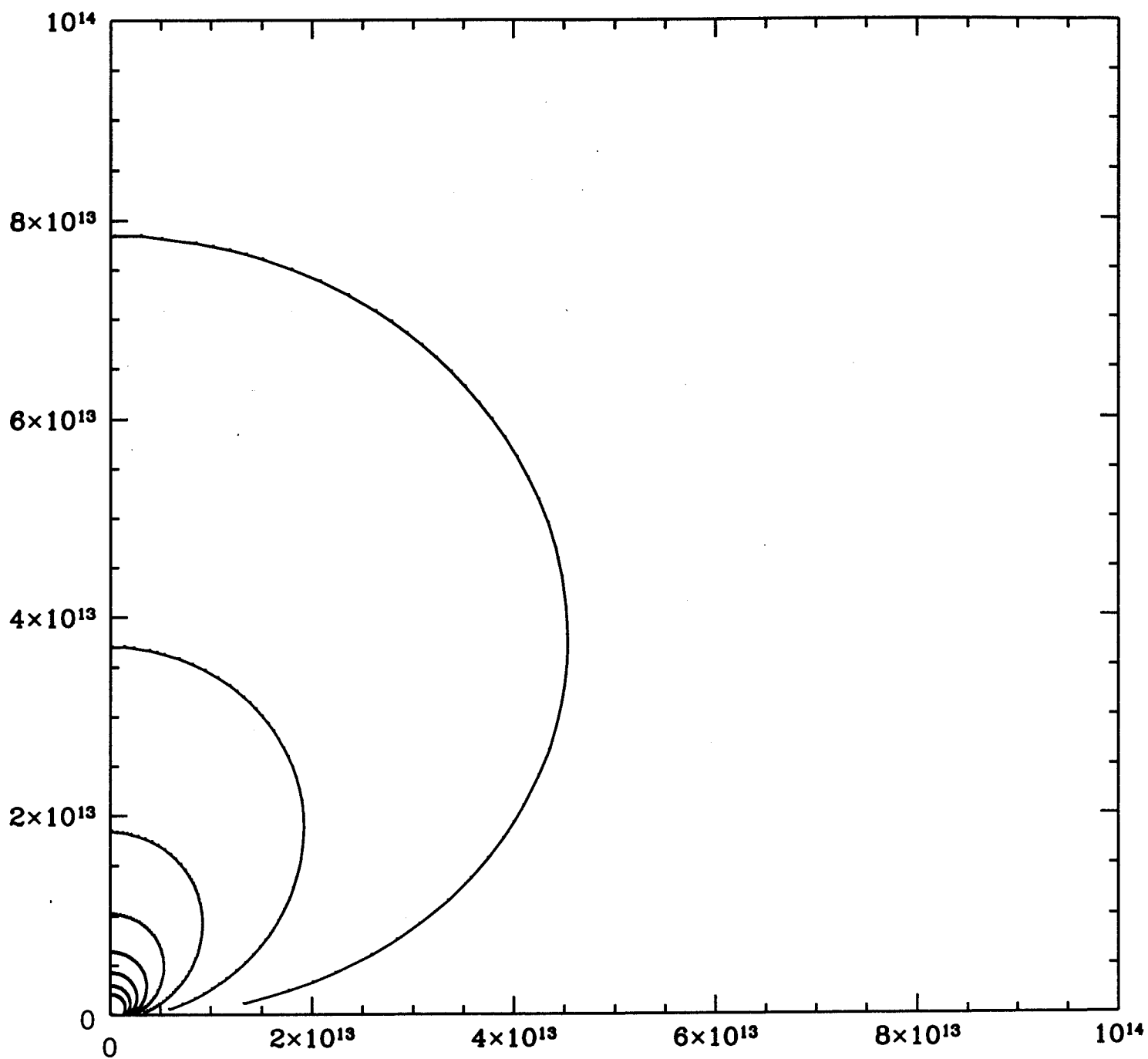


Fig 3

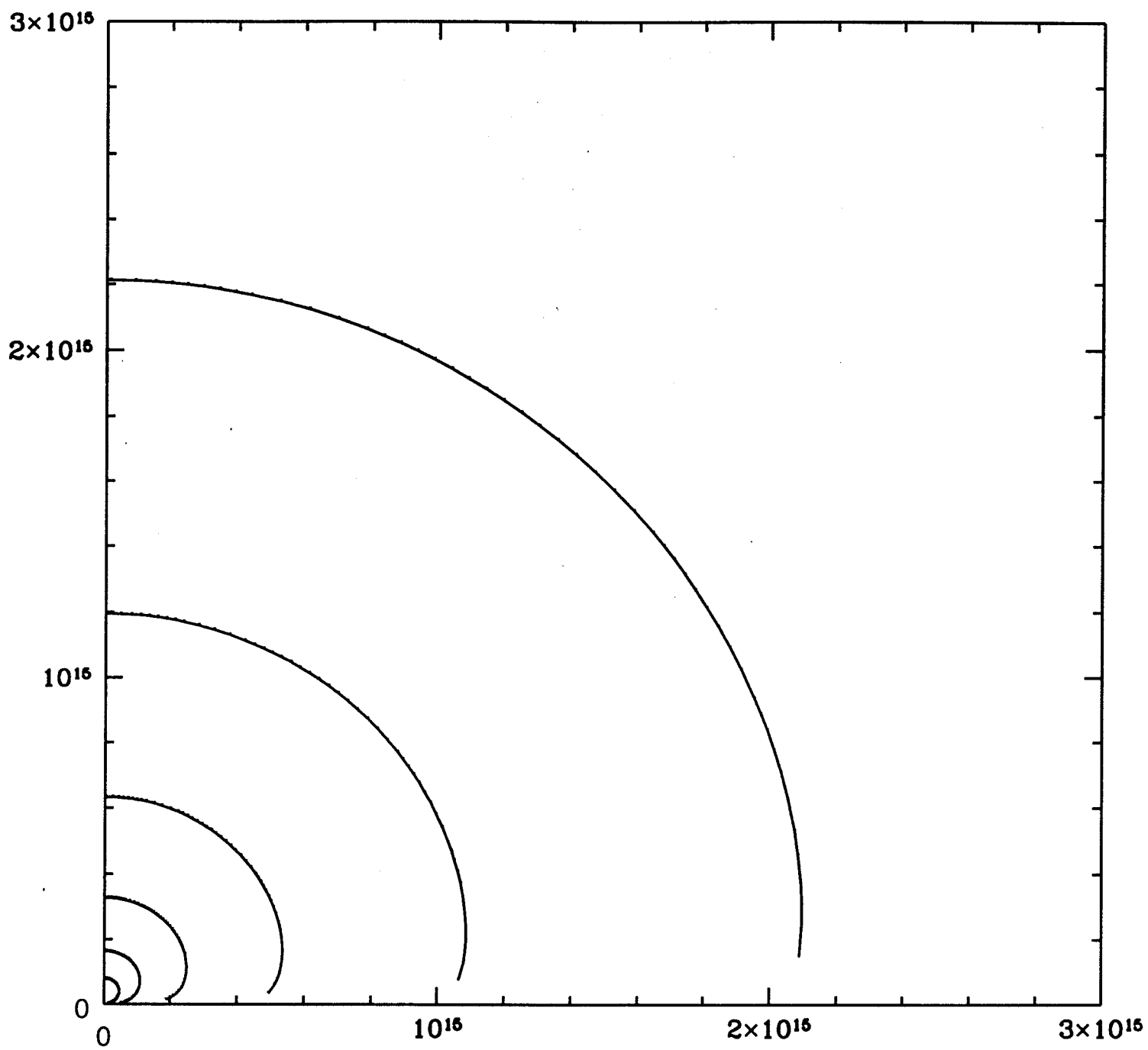


Fig 4

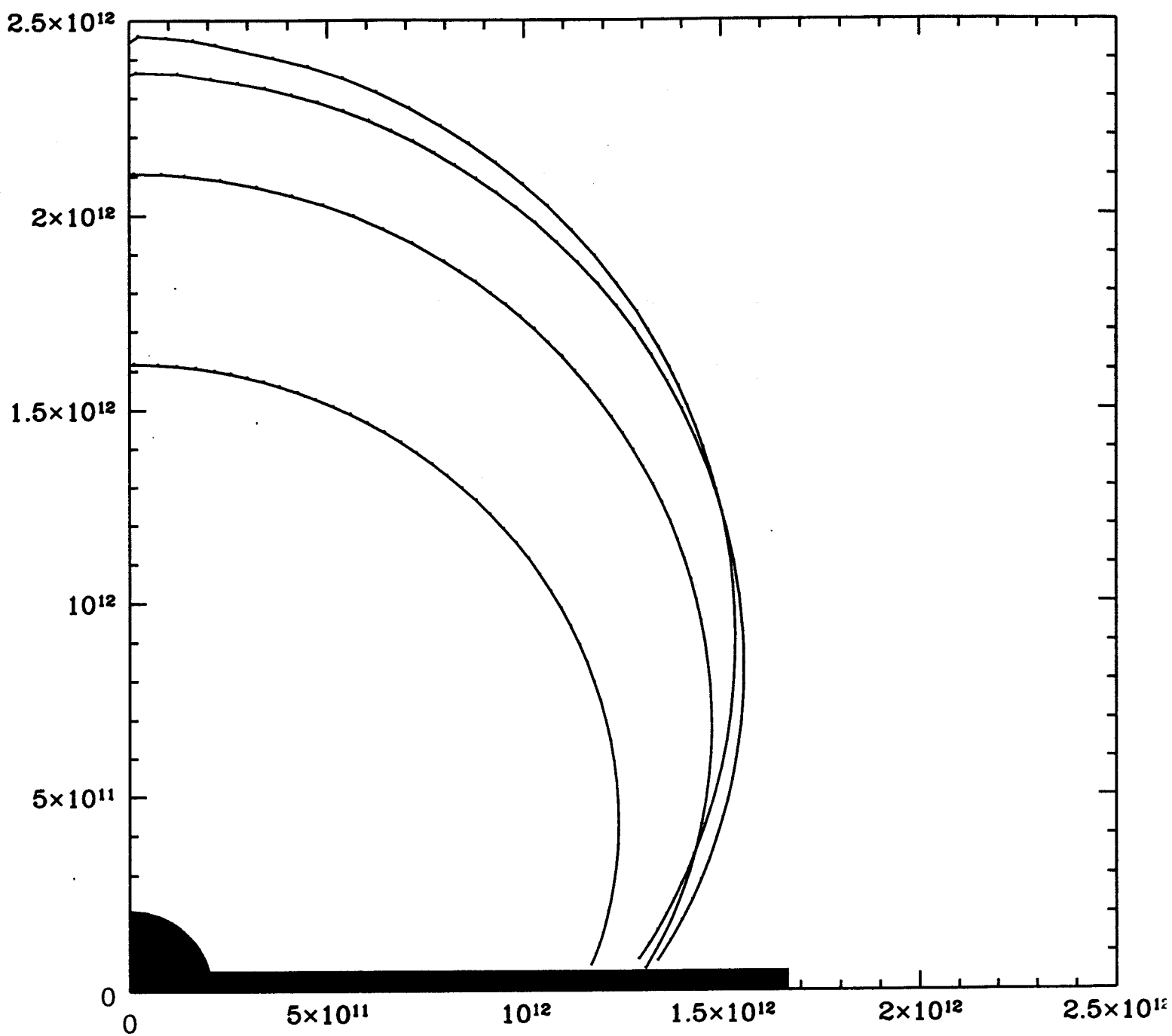


Fig 5

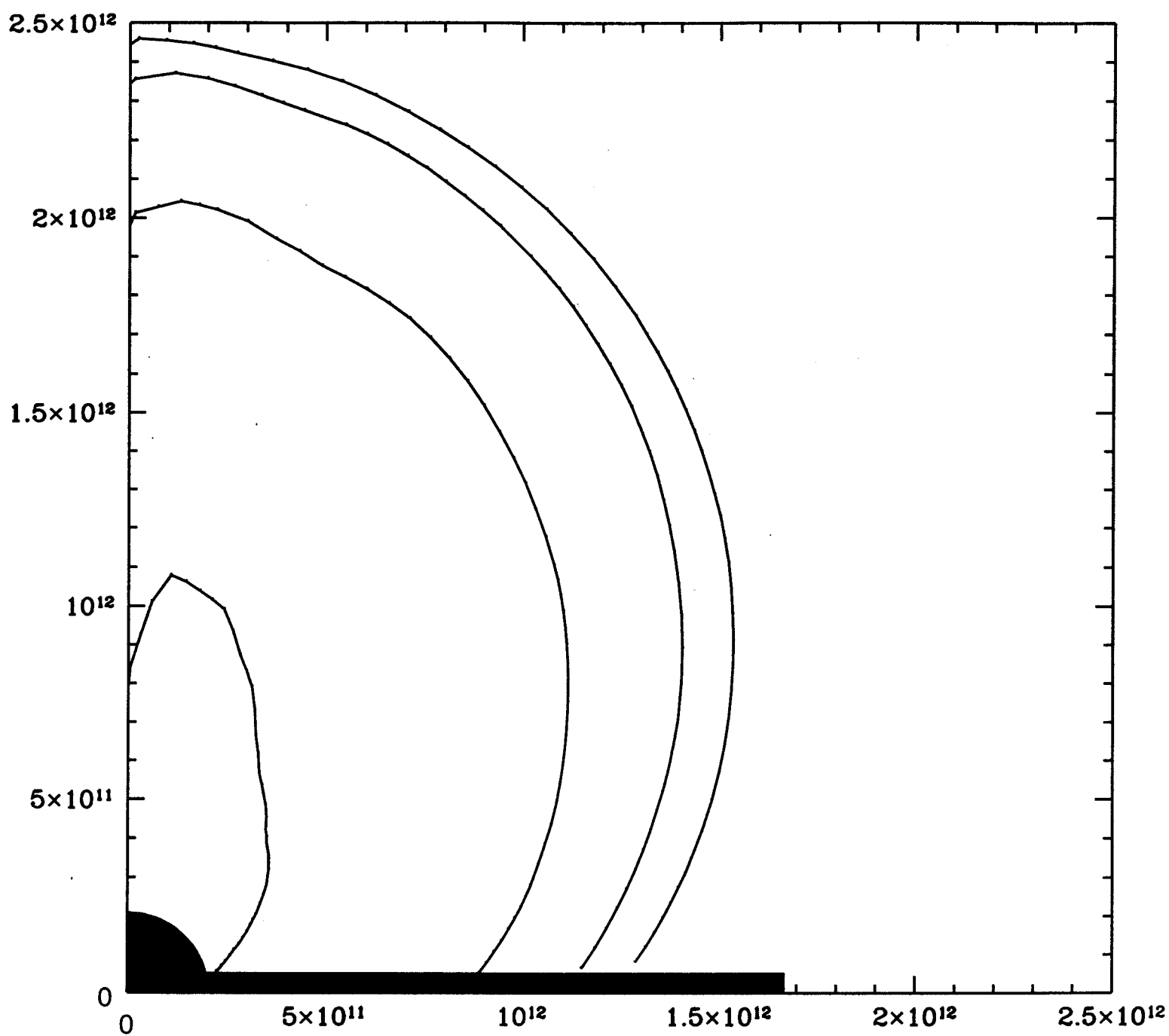


Fig 6

FIGURE 1. Minimum breakout wind speed versus evolutionary time. The three loci correspond to three ratios of the wind mass loss to infall accretion rate $\alpha = \dot{M}_{wind}/\dot{M}_{infall}$. For a given α , the region above the curve corresponds to breakout, while that below the curve corresponds to recollapse. From top to bottom, we have $\alpha = 1/30, 1/10, 1/3$. At early times, the infall is nearly spherical, which increases the required speed. The increase in required wind speed at late times is associated with the increased gravitating mass of the protostar. See text for the dimensional units used.

FIGURE 2. Time-Evolution of an escaping shell (early evolution), corresponding to $\alpha = 0.1$, $\nu = 4.2$, and $\tau = 2.0$. The critical wind speed for these parameters is $\nu_{crit} = 3.95$. The shapes correspond to equal time intervals of 0.024 years. The subsequent evolution of this shell is shown in the next two figures on a larger scale. The scale of the centrifugal radius is indicated by the disk. Lengths are in cm.

FIGURE 3. Time-Evolution of an escaping shell (further evolution), corresponding to the same parameters as Figure 2 but for with increasing times steps and on a larger scale. The innermost curve of this figure is the same as the innermost of that Figure. However, the elapsed time increases by a factor of two with each curve: 1,2,4,8,16 and 32 time units.

FIGURE 4. Time-Evolution of an escaping shell (late time), corresponding to the same parameters as Figures 2 and 3. Here the shell has gone well beyond the centrifugal radius of the infall and is in the increasingly spherically symmetric infall region. Hence the shell becomes more spherical as

it sweeps up this material. The elapsed time doubles with each successive curve. The innermost here is the same as the outermost of Figure 3 (128 time units), while the outermost is greater by a factor of 32 (4096 time units). The final time corresponds to 99.5 years since launch.

FIGURE 5. Time-Evolution of a re-collapsing shell (rising phase), corresponding to $\alpha = 0.1$, $\nu = 3.7$, and $\tau = 2.0$. Shown for equal time intervals of $1/4$ the time to reach the highest point. Note that this is the same interval as the unit used in Fig. 2. The critical wind speed at this time is $\nu = 3.95$. Lengths are in cm. The recollapse is shown in Figure 6.

FIGURE 6. Time-Evolution of a re-collapsing shell (falling phase), corresponding to $\alpha = 0.1$, $\nu = 3.7$, and $\tau = 2.0$. Shown for equal time intervals of $1/4$ the time to reach the highest point. The critical wind speed at this time is $\nu = 3.95$. The largest shell is that at the turn-around, and successive times have smaller radius as the shell accelerates inward under the force of gravity. For the reference values of section 5, the dimensional time is 77,000 years, and the wind speed is 352 *km/s*.